Gadolinium-enhanced magnetic resonance angiography of abdominal aortic aneurysms

Martin R. Prince, MD, PhD, Dasika L. Narasimham, MD, James C. Stanley, MD, Thomas W. Wakefield, MD, Louis M. Messina, MD, Gerald B. Zelenock, MD, William T. Jacoby, MD, M. Victoria Marx, MD, David M. Williams, MD, and **Kyung J. Cho, MD,** *Ann Arbor, Mich.*

Purpose: **The objective of this study was to assess the usefulness of gadolinum-enhanced magnetic resonance angiography (MRA) for defining anatomic features relevant to performing aortic surgery for aneurysmal disease.**

Methods: **Anatomic data defined by MRA, including abdominal aortic aneurysm (AAA) size and character, as well as the status of the celiac, mesenteric, renal, and iliac arteries, were correlated with angiography, ultrasonography, computed tomography, or operative data in 43 patients. Five MRA sequences were obtained in an hour-long examination optimized for aortoiliac, splanchnic, and renal artery imaging at 1.5 T in a body coil. Four of the sequences were performed during or after infusion of gadolinium to improve image quality.**

Results: **MRA correctly defined the maximum aneurysm diameter, as well as its proximal and distal extent in all patients. MRA detected 33 of 35 significant stenoses among 153 splanchnic, renal, or iliac branches examined (sensitivity = 94% and specificity = 98%). MRA did not resolve the degree of aortic branch stenotic disease sufficiently to precisely grade its severity. MRA did not reliably define the status of the inferior mesenteric artery, lumbar arteries or internal iliac arteries. One ruptured AAA and one inflammatory AAA were correctly diagnosed by MRA. No patient had a contrast reaction or contrast-induced renal toxicity related to administration of gadolinium.**

Conclusion: **Gadolinium-enhanced MRA of AAA provides appropriate, essential anatomic information for aortic reconstructive surgery in a 1-hour examination devoid of contrast-related renal toxicity or catheterization-related complications attending conventional arteriography. (J VASC SURG 1995;21:656-69.)**

Magnetic resonance imaging (MRI) has evolved over the past decade to become an accepted technique to obtain images of the abdominal aorta and abdominal aortic aneurysms (AAA).[1-5] Advances in MRI for vascular imaging, known as magnetic resonance angiography (MRA), have enabled the additional evaluation of aortic branch vessels.[6-11] However, limitations in MRA imaging of the slow, swirling flow within aneurysms, turbulent flow in stenoses, and tortuous iliac arteries[12-14] have limited the usefulness of these general studies in providing detailed information necessary for preoperative planning.

From the Departments of Radiology and Surgery (Drs. Stanley, Wakefield, Messina, and Zelenock), University of Michigan, Ann Arbor.

This research was funded in part by NIH grant no. HL46384 and by an RSNA award.

Reprint requests: Martin R. Prince, MD, University Hospitals B2B311G, 1500 E. Medical Center Dr., Ann Arbor, MI 48109-0030.

0741-5214/95/$3.00 + 0 **24/1/63164**

Recent developments in gadolinium-enhanced MRA have overcome many preexisting imaging problems.[15-18] Gadolinium, a paramagnetic contrast agent, shortens the T_1 (spin-lattice) relaxation time of blood, making blood distinct from surrounding tissues regardless of its flow rate or direction. The technique provides true anatomic images that have an appearance similar to conventional or digital subtraction contrast arteriograms (hereafter referred to as angiography). This study describes a combination of one spin-echo and four gadolinium-enhanced MRA sequences whose potential to resolve imaging issues associated with the preoperative evaluation of abdominal aortic aneurysms was assessed in 43 patients.

MATERIAL AND METHODS

Patients. Forty-three consecutive patients, 31 men and 12 women, underwent gadolinium-enhanced MRA of AAA from November 1993 through November 1994. Patients ranged in age from 36 to 87 years (mean 70 years). Twenty patients were at increased risk for exposure to iodinated

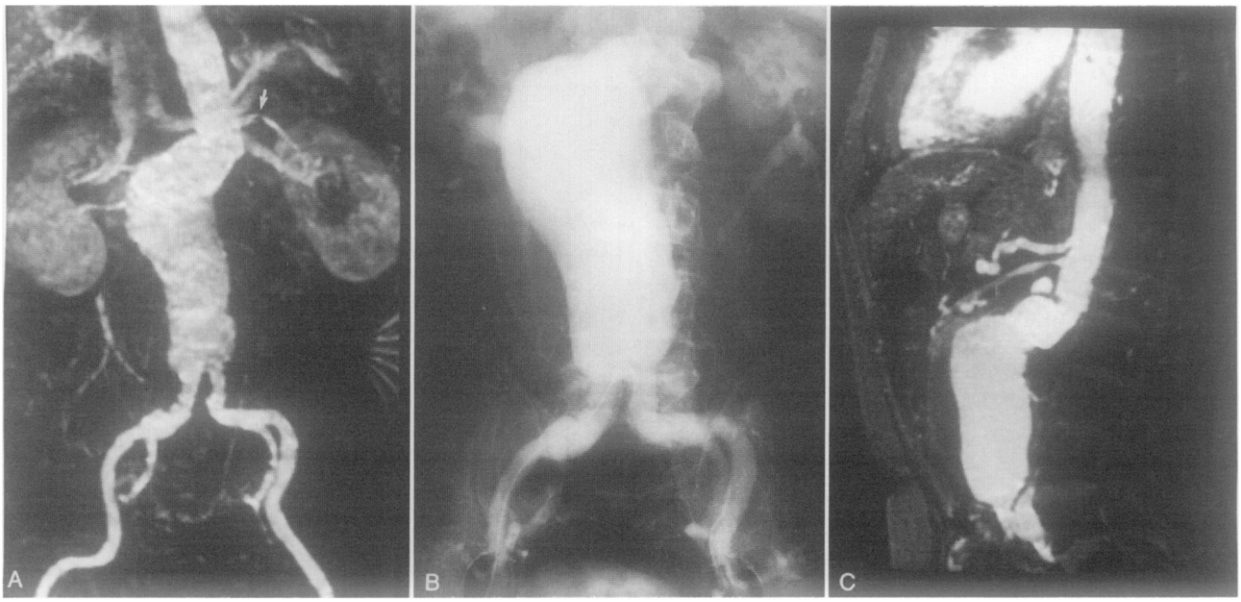

Fig. 1. A, Coronal MIP of dynamic gadolinium-enhanced 3D MRA of AAA. Preferential enhancement of arteries allows evaluation of iliac arteries without confounding effects of overlapping veins. However, there is moderate enhancement of renal, splenic, and portal veins). Note left renal artery stenosis *(arrow)*. **B,** Conventional aortogram. **C,** Sagittal 2D time-of-flight MRA after gadolinium infusion shows same AAA with thrombus anteriorly, normal preaortic left renal vein, normal celiac trunk, and moderate stenosis of superior mesenteric artery.

contrast. Eighteen had concomitant renal insufficiency with a mean serum creatinine of 3.1 mg/dl (range 1.7 to 7.8 mg/dl). Two patients had known major allergic reactions to iodinated contrast.

Imaging technique. Imaging was performed on a 1.5 T magnet (GE Medical Systems, Signa, Milwaukee, Wis.) with use of the body coil. The imaging sequences included sagittal T_1 (9:36 minutes), coronal three-dimensional (3D) spoiled gradient echo during infusion of 42 or 63 ml gadolinium chelate (3:20 minutes), Sagittal two-dimensional time-of-flight (4 minutes), axial two-dimensional time-of-flight (10 minutes), and axial three-dimensional phase contrast (13:07 minutes) images. The specific imaging parameters, details about the gadolinium infusion timing, and methods of image reconstruction are described for others considering use of this technology (see appendix).

MR images were independently analyzed by two vascular radiologists blinded to the findings at angiography, surgery, and computed tomography (CT). Any disagreements in interpretation were resolved by consensus. Aneurysms were classified as suprarenal (aneurysmal above the renal arteries), pararenal (aneurysm at level of renal arteries but not higher), juxtarenal (origin of aneurysm at or within 1 cm below renal arteries), or infrarenal (origin of aneurysm more than 1 cm below renal arteries). The distal extent was defined as the first point inferior to the aneurysm that was near-normal caliber. The maximum aneurysm diameter was measured electronically on the MR computer monitor from its outer-to-outer wall margins. Thrombus, when present, was noted. The celiac, proximal superior mesenteric, renal, common iliac, external iliac, and internal iliac arteries were graded as normal, mildly diseased (less than 50%), moderately stenotic (50% to 75%), severely stenotic (greater than 75%), or occluded.

MR images were also evaluated for evidence of aortic dissection, inflammatory changes and aortic rupture. Aortic dissection was defined as having an intimal flap or medial separation. Inflammatory aneurysm was defined as having surrounding enhancing tissue. Ruptured aneurysm was defined as having an aortic mural defect and a retroperitoneal collection with MRA features of hemorrhage.

Angiography, ultrasonography, computed tomography, and operative correlations. MRA findings were compared with those at angiography (11 patients), ultrasonography (10 patients), CT (11 patients), and at operation (25 patients). Operative findings were determined by review of the operative notes and interviews with each surgeon. Operative correlation for grading the severity of occlusive lesions was only used when the surgeon was confident in the assessment of the vascular segment on the basis of evaluation by probe, Doppler scanning, or visual inspection. Angiographic, ul-

Fig. 1. D-F., Conventional lateral aortogram confirms MRA findings. **E,** Oblique axial reformation shows proximal renal arteries with moderate left renal artery stenosis *(arrow)* confirmed by **(F)** conventional digital subtraction angiography.

trasound, and CT findings were obtained by retrospective review of reports. Findings at operation and angiography were considered gold standards. For calculations of sensitivity and specificity, stenotic lesions were classified positive (significant) when graded as moderate, severe, or occluded and were classified negative (not significant) when graded as mild.

RESULTS

Extent of AAA. The MR classification of the aneurysm and evaluation of its distal extent were correct in all 28 patients having surgical or angiographic data for correlation. The gadolinium-enhanced MRI sequences demonstrated 11 suprarenal, six pararenal, six juxtarenal, and 20 infrarenal AAAs (Fig. 1). Aneurysmal dilation of the thoracic aorta affected nine patients. Aneurysms terminated at or above the aortic bifurcation in 21 patients, extended into the iliac arteries in 18 patients (Fig. 2), and terminated at the proximal anastomosis of existing aortoaortic or aortofemoral grafts in six patients. One patient with an aortoaortic graft exhibited a saccular aneurysm just below the distal anastomosis (Fig. 3).

Size of AAA. AAA diameters, as assessed by MRA, ranged from 3.0 to 8.7 cm (mean = 5.4 cm). Aneurysm size, as measured by MRA, was within 3 mm of the CT measurements in all eleven patients in whom CT correlation was available within 3 months of MRA (Fig. 4). MRA and ultrasound AAA diameter measurements were within 5 mm in all 10 patients in whom ultrasonography was performed

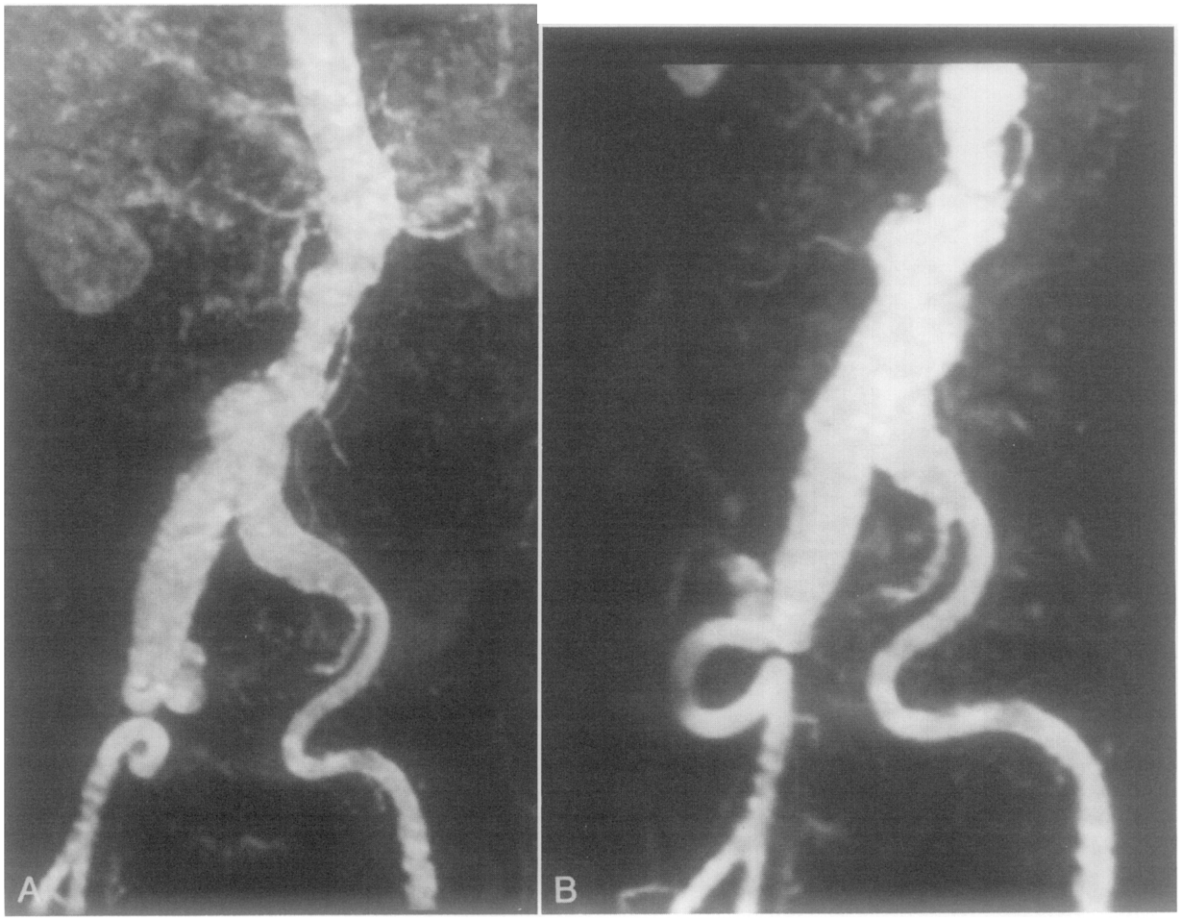

Fig. 2. Coronal and oblique coronal MIP images (**A** and **B**) of aneurysmal changes in aorta and common iliac arteries with visualization of extremely tortuous external iliac arteries.

within 3 months before surgery, except one. This one patient had a 7.3 cm suprarenal aneurysm detected by MRI that was not assessed by ultrasonography. For the infrarenal segment of this aneurysm, the MRA and ultrasound diameter measurements were within 3 mm.

Character of AAA. An inflammatory AAA was evident on MRA in one patient with a thick enhancing wall of the aneurysm (Fig. 5). A ruptured aneurysm was identified by MRA in another patient (Fig. 6). Emergency operation confirmed the presence of a contained rupture. This patient had a serum creatinine level greater than 5 mg/dl with bilateral renal artery stenoses noted on MRA. He was treated successfully with a Dacron aortoaortic interposition graft and bilateral aortorenal bypasses. A third patient had a type III aortic dissection extending into the common iliac arteries (Fig. 7). There were no false-positive or false-negative determinations of aortic rupture, aortic dissection, or inflammatory aneurysm. This technique was 100% sensitive and 100% specific for these observations in this series.

Associated findings. Thirty aneurysms, in addition to the aortic aneurysms were identified at angiography (n = 6), at operation (n = 20), or at both angiography and operation (n = 4). These included 23 involving the common iliac arteries, five involving internal iliac arteries, and two involving the common femoral arteries. MRA indentified all 30 of these aneurysms (sensitivity = 100%). There was a single false-positive determination of aneurysm. This occurred in a patient with an aneurysmal right common iliac artery and an ectatic left common iliac artery determined by angiography, who was believed to have bilateral common iliac artery aneurysms determined by MRA.

MRA detected a total of 89 aortic branch occlusive lesions characterized as moderately stenotic (n = 45), severely stenotic (n = 31), or occluded (n = 13) among a total of 430 vascular segments

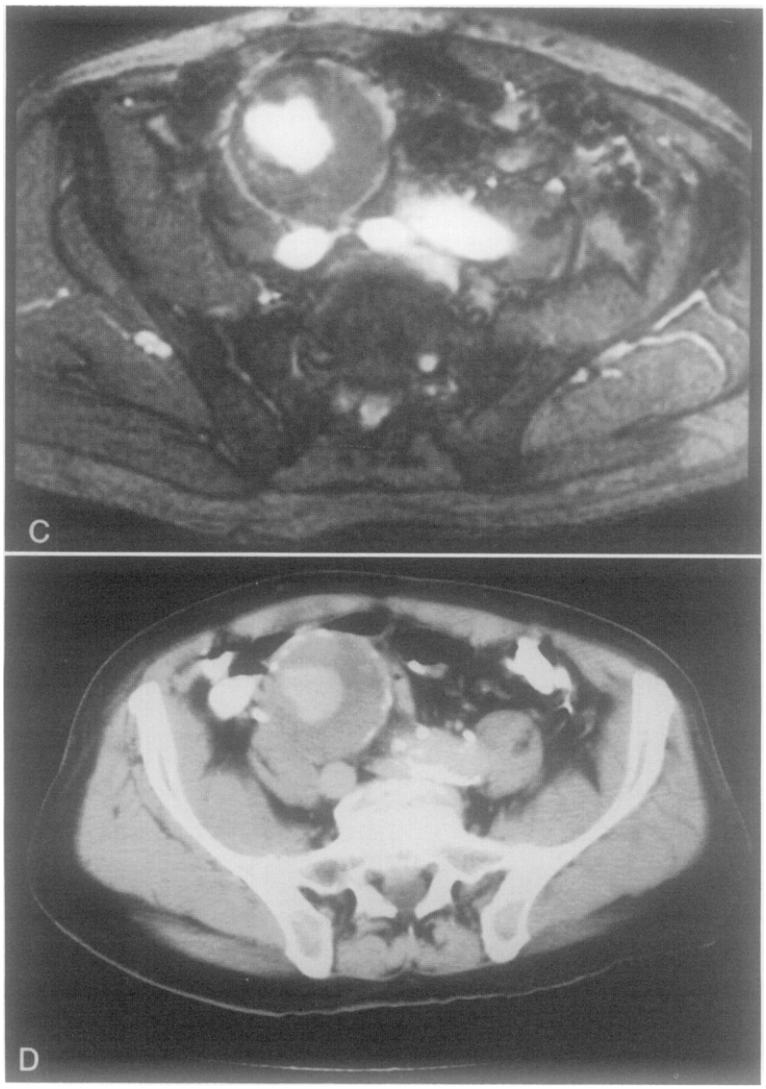

Fig. 2. C, D. Axial 2D time-of-flight post-gadolinium image at level of common iliac arteries shows extensive intraluminal thrombus within iliac aneurysm that is confirmed by **(D)** CT. Note that extensive calcified plaque observed in left common iliac artery on CT **(D)** is not seen on corresponding MR angiogram **(C).**

imaged in the series of 43 patients. In grading these 430 vascular segments, there was agreement between the two MRA readers in 377 segments (88%). All cases of disagreement were never by more than a single grade. The stenotic vessels involved included the celiac (n = 19), superior mesenteric (n = 4), renal (n = 32), and iliac (n = 34) arteries.

Angiographic or operative correlations were possible for 153 of the vascular segments in 28 patients. In these vascular segments with correlation, MRA identified 33 significant occlusive lesions (Fig. 8). When splanchnic, renal, and iliac artery occlusive lesions graded as moderate or worse were considered positive, the sensitivity was 94%, and the specificity was 98% for MRA detection of these lesions. MRA provided inconsistent images of distal renal arteries and their intraparenchymal branches. The mean length of the renal artery imaged by MRA was 6.3 ± 2.0 cm on the right and 5.6 ± 2.6 cm on the left. One renal artery could not be evaluated by MRA because its origin was obscured by a surgical clip artifact related to a prior aortic reconstructive procedure. MRA did not reliably obtain images of the inferior mesenteric arteries or lumbar arteries. The more distal superior mesenteric artery, celiac artery, and internal iliac artery branches were not imaged by

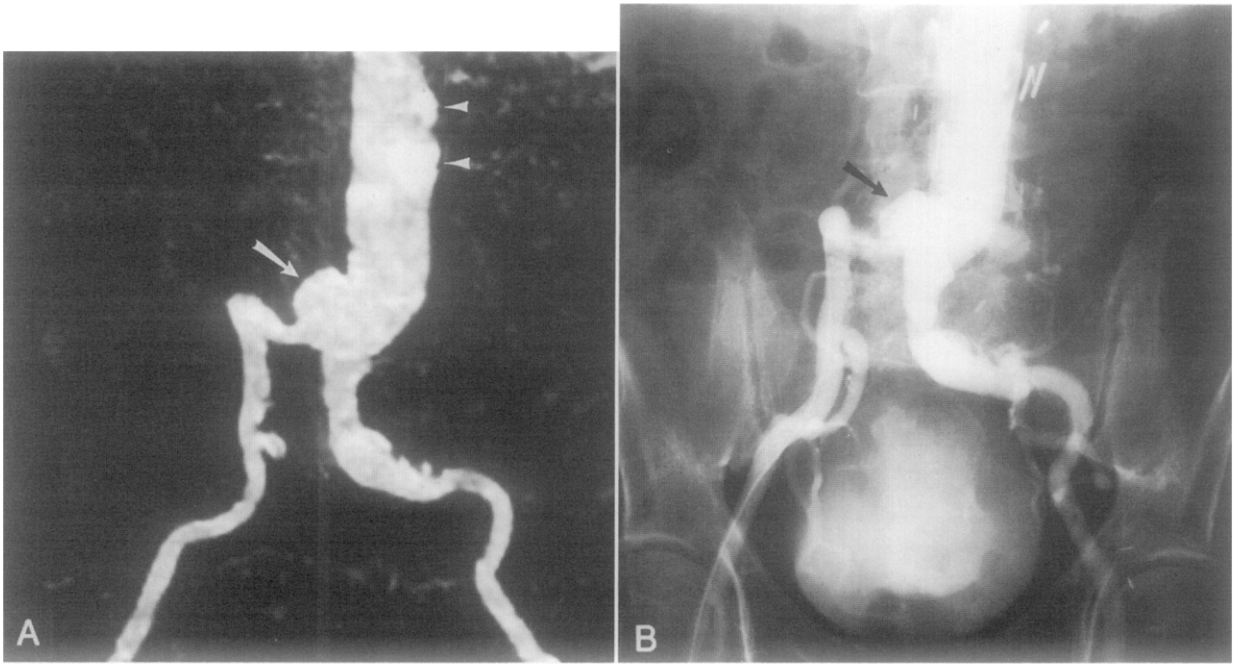

Fig. 3. A, Coronal MIP image of infrarenal aortoaortic graft with recurrent saccular aneurysm *(arrow)* just below graft distal anastomosis. Note surgical clip artifacts *(arrowhead)*. **B,** Conventional angiogram confirms MRA findings.

MRA because they extended beyond the 3D imaging volumes used in these examinations.

MRA identified three accessory renal arteries. Two additional accessory renal arteries were missed by both MRA and angiography. One of these was found at operation with proximal occlusion. It was not evident on MRA even in retrospect or on a remote angiogram obtained 1 year previously. The other was discovered in retrospect on both the MRA and the angiogram when the patient had development of a small lower pole renal infarct after operation.

Normal, preaortic left renal veins were identified in 34 patients (Fig. 1, *C*). Four patients had circumaortic left renal veins and two patients had retroaortic left renal veins. The left renal vein was not identified in two patients who had undergone a prior left nephrectomy and in a third patient with marked atrophy of the left kidney. In 28 patients having either operative or CT correlation, the MRA assessment of left renal vein anatomy was confirmed in all but two patients. These two patients both had circumaortic left renal veins on the basis of the MRA, but the surgical team did not specifically look for the retroaortic vein and could not confirm its presence.

Thrombus was present in the AAA of 35 patients (81%). Thrombus was evident in all 27 aneurysms

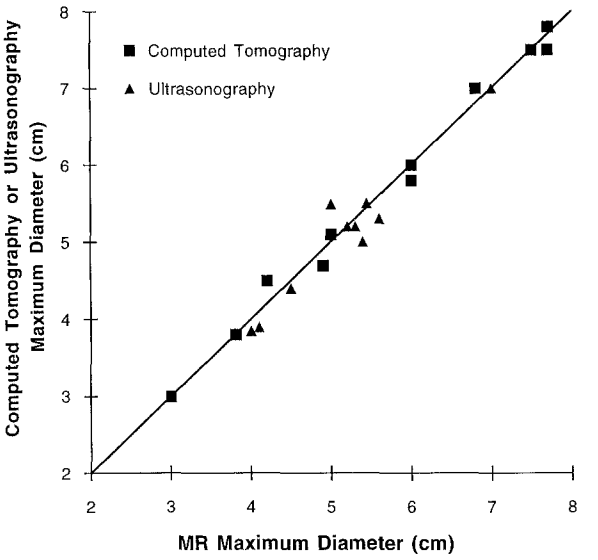

Fig. 4. MRA AAA diameter measurements versus CT *(square)* and ultrasound *(triangle)* AAA diameter measurements. *Solid line* corresponds to perfect agreement.

greater than 5 cm in maximum diameter and tended to be evident in the regions of maximum aneurysm diameter (Fig. 1, *C*). In contrast, only seven of 15 aneurysms (47%) measuring 4.5 cm or less in maximum diameter had thrombus. In all 29

Fig. 5. A, Axial and **B,** sagittal 2D time-of-flight image obtained after gadolinium infusion shows extensive infiltration/enhancement of preaortic tissue *(arrows)* consistent with inflammatory aneurysm that was confirmed at operation.

patients with either CT or surgical correlation, the assessment of thrombus by MRA was corroborated. Angiography did not reliably demonstrate thrombus.

Seven patients exhibited important MRA findings not related to their AAA. One patient had a large retroperitoneal mass with MRA features of fat and hemorrhage, which was identified as a liposarcoma at biopsy. Another patient had an enhancing lesion in the spinal cord believed to be suspicious for a metastasis. Another patient had massive splenomegaly correctly identified by MRA but also had a 5 cm mass at the base of the mesentary not detected prospectively on the MRA and found by surgical

biopsy to be lymphoma. This mass was difficult to identify on the MRA, even retrospectively, because it was similar in appearance to loops of bowel. One other patient had a severe L1 vertebral compression fracture. Two patients had liver lesions with imaging features consistent with benign hemangiomas. Numerous patients had incidental renal cysts or evidence of degenerative changes in the spine.

All patients tolerated the MRI well except for two with claustrophobia. Claustrophobia was not a problem in any patient administered diazepam, 5 to 10 mg parenterally. Two patients had to be restudied because of technical problems. There were no contrast reactions. Data on periexamination serum creatinine levels were available in 18 patients who were monitored for their renal insufficiency. The average serum creatinine level in these 18 patients was 3.5 mg/dl on the day of or day before the MRA study and 3.4 mg/dl the next day. No patient had a rise in serum creatinine attributable to gadolinium. There were no local complications from the gadolinium infusion.

DISCUSSION

Imaging of an AAA in preparation for aortic reconstructive surgery varies from center to center based on the patient's clinical presentation, proximity of the aneurysm to the splanchnic and renal arteries, presence or absence of lower extremity vascular occlusive symptoms, concomitant illnesses, such as hypertension or renal insufficiency, and personal preferences of the surgeons. Ultrasonography is generally used in monitoring patients with AAA and screening patients suspected of having AAA.[19,20] Because ultrasonography is noninvasive and relatively inexpensive and gives reliable diameter measurements, it is useful for these purposes, but it is not adequate in providing detailed information about the aortic anatomy. Angiography is considered essential when the superior extent of the AAA is at or above the renal vessels and when concomitant splanchnic, renal, or iliofemoral arterial stenotic or aneurysmal lesions are suspected.[21-24] Cross-sectional imaging by CT has been claimed to be superior to angiography in evaluating the aneurysm diameter, the location of the left renal vein, and other associated anomalies of the kidneys and retroperitoneum.[25]

However, CT studies require large volumes of iodinated contrast and do not adequately evaluate the presence or absence of significant arterial occlusive disease.[26] Recently, helical CT has shown potential for evaluating aortic branches, but its field-of-view is limited when the collimation is made narrow enough to evaluate renal arteries and calcified plaques can obscure stenoses.[27] In practical terms, no contemporary single imaging technique adequately provides all of the necessary anatomic details required for planning aortic reconstructions in patients with AAA. More than one imaging study is commonly performed in most clinical practices.

Fig. 6. Coronal MIP of leaking AAA. Contained rupture at left margin of aneurysm *(arrow)* was confirmed at emergency operation.

This investigation describes a combination of MRI sequences, obtained in a single 1-hour study, that can obtain anatomic data needed to plan operative interventions in patients with an AAA. The existing limitations of standard time-of-flight and phase contrast MRA techniques have been overcome by use of gadolinium, a paramagnetic contrast agent.[15-17] The gadolinium improves image quality by facilitating T_1 relaxation wherever it is concentrated. The high concentration of gadolinium in blood thus results in increased vascular signal on any image with T_1 weighting, including gradient echo, time-of-flight, and phase contrast. In this study, the improvement in image quality was substantial (Figs. 1-9). Because vascular contrast in these images was based on T_1 relaxation instead of blood flow,

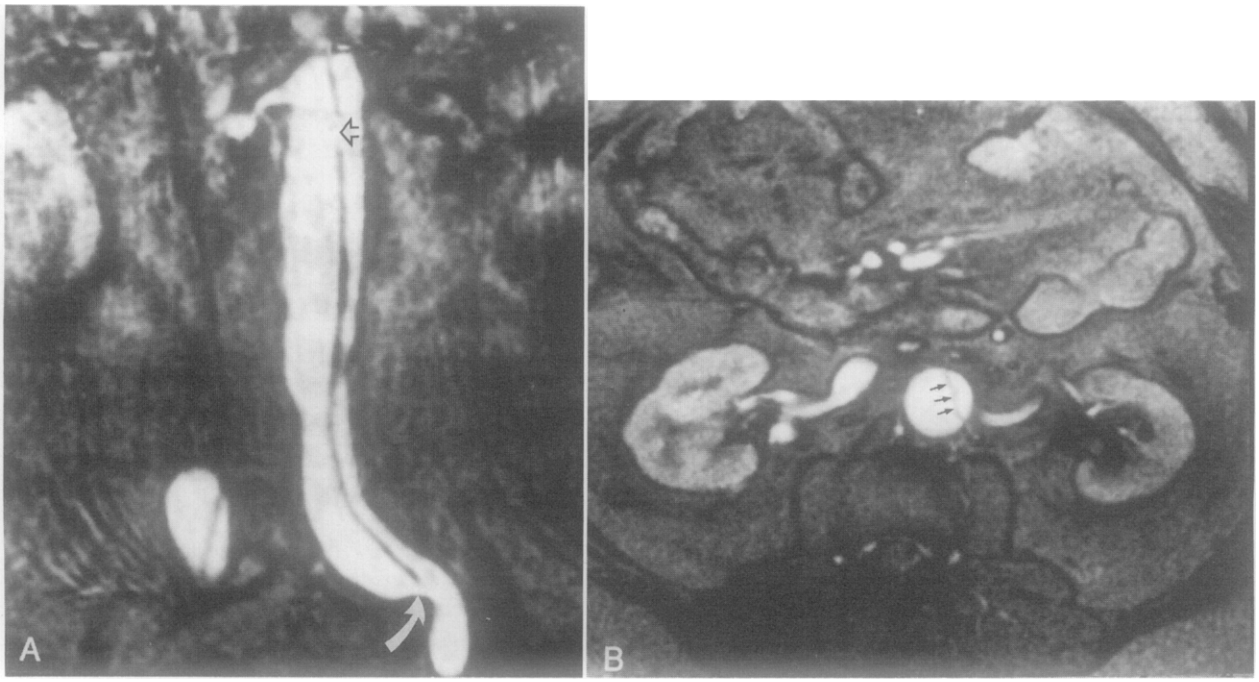

Fig. 7. A, Coronal MIP shows dissection involving abdominal aorta and common iliac arteries. Large reentry tears are seen at level of renal arteries *(open arrow)* and in left common iliac artery *(curved arrow)*. **B,** Intimal flap also well seen at level of the left renal artery on axial 2D time-of-flight image obtained after gadolinium *(arrows)*.

most of the common MRA flow artifacts were eliminated.

Gadolinium is a heavy metal administered after being chelated to diethylenetriaminimepentaacetic acid, as are other heavy metals used for imaging, such as technetium. In its chelated form, gadolinium is excreted by the kidneys with a serum half-life of approximately 1.5 hours. It has no known significant side effects and no nephrotoxicity, and thus it is safe for use in patients with renal insufficiency.[28,29] This potential for a contrast arterial examination without nephrotoxicity is especially important for the preoperative evaluation of patients with complex disease involving the renal circulation. The kidneys in these patients should not be exposed to large quantities of iodinated contrast immediately before procedures that may involve further renal insults with blood loss and hypotension, as well as kidney ischemia caused by renal artery or suprarenal aortic cross-clamping. There is no reason to delay operative intervention after gadolinium-enhanced MRA as has been the practice at the authors' institution after conventional arteriography with iodinated contrast. Gadolinium also has a low incidence of allergic reactions and does not cross-react with iodinated contrast. Thus it is safe for patients with a history of allergic reaction to iodinated contrast.

A complete evaluation of AAA requires a combination of multiple MRI sequences: (1) The initial sagittal T_1 sequence defines the location of the aneurysm, as well as renal and splanchnic arteries for planning the higher resolution gadolinium-enhanced sequences. It shows the approximate size of each kidney, the size of the aneurysm, and identifies the location of the left renal vein. (2) The dynamic gadolinium-enhanced 3D volume can be reconstructed in coronal and sagittal projections to produce images that are similar to biplane aortography. These images are best for evaluating the renal and splanchnic artery origins, the iliac arteries, and the distal extent of the aneurysm. (3 and 4) The sagittal and axial 2D time-of-flight images demonstrate the maximum size of the aneurysm, its proximal extent, perianeurysm inflammation, the presence of thrombus, and the features of the thrombus, including location, surface irregularity or enhancement. (5) The phase contrast images define the renal arteries in greater detail to allow grading the severity of occlusive lesions. This combination of gadolinium-enhanced MRA sequences yielded a higher accuracy

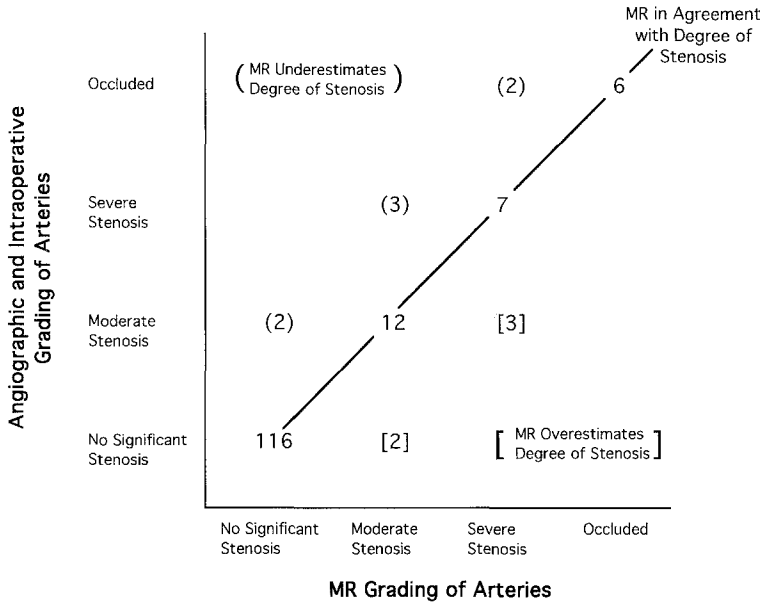

Fig. 8. Grading of visceral and iliac arterial stenoses by MRA compared with angiography and intraoperative evaluation. MRA grading matched other grading in 141 arteries and was off by one grade in 12 arteries. Overall sensitivity for detecting significant stenoses was 33 of 35 (94%), and specificity was 116 of 118 (98%).

for detecting and grading occlusive lesions than has been described in previous MRA studies.[5-18]

Although the gadolinium MRA image resolution was not equal to conventional angiographic examination results, in some aspects gadolinium MRA was superior to angiography. Because the entire arterial blood pool contains gadolinium, aneurysms are seen with high contrast in their entirety on a single large field-of-view image (Fig. 1). This often is not possible with angiography unless large volumes of iodinated contrast are used. Gadolinium MRA provides cross-sectional images in any plane. This allows accurate measurement of aneurysm size and interrogation of all major abdominal branch origins with a single injection. Reformations of the three-dimensional data provide images of the origins of the aortic branch vessels that may not be possible with conventional biplane aortography when arteries overlap the aneurysm in a convoluted pattern. This is particularly useful for evaluating the relationship of the renal arteries to the AAA neck in complex cases.

Thrombus is readily identified by MRA. Although this information is not important for conventional AAA operations, assessment of intraluminal thrombus may become important in planning endoluminal stent graft placement as the latter technology is introduced into clinical practice. Additional features of thrombus, such as enhancement and surface character that may relate to its embolic potential, can be evaluated by MRA. Furthermore, the axial and sagittal images (Figs. 1, *C*, 5) allow accurate aorta diameter and length measurements that may facilitate customization of an endoluminal graft for a given AAA.

Although it is conceptually similar to spiral CT,[27] gadolinium-enhanced 3D MRA has the advantages of not using iodinated contrast, not exposing the patient to ionizing radiation, and requiring less critical timing of the contrast infusion. The images are acquired in the plane of the aorta, allowing 3D gadolinium MRA to cover a much greater length (typically 36 cm) of aorta with high-resolution ($2.5 \times 1.4 \times 1.4$ mm) in a single infusion. Interestingly, respiratory motion is not as great a problem with MRA as it is with spiral CT. High-quality MRA is routinely obtained in patients who cannot hold their breath for the 30 seconds required for spiral CT. The cost of the gadolinium is comparable to the cost of the nonionic contrast used for spiral CT. Extravasation of gadolinium during infusion is not a serious complication.

Gadolinium-enhanced MRA provided sufficient anatomic detail to detect all aneurysms and all relevant major branch vessel abnormalities documented at angiography and operation in this clinical study. The failure of MRA to evaluate the inferior

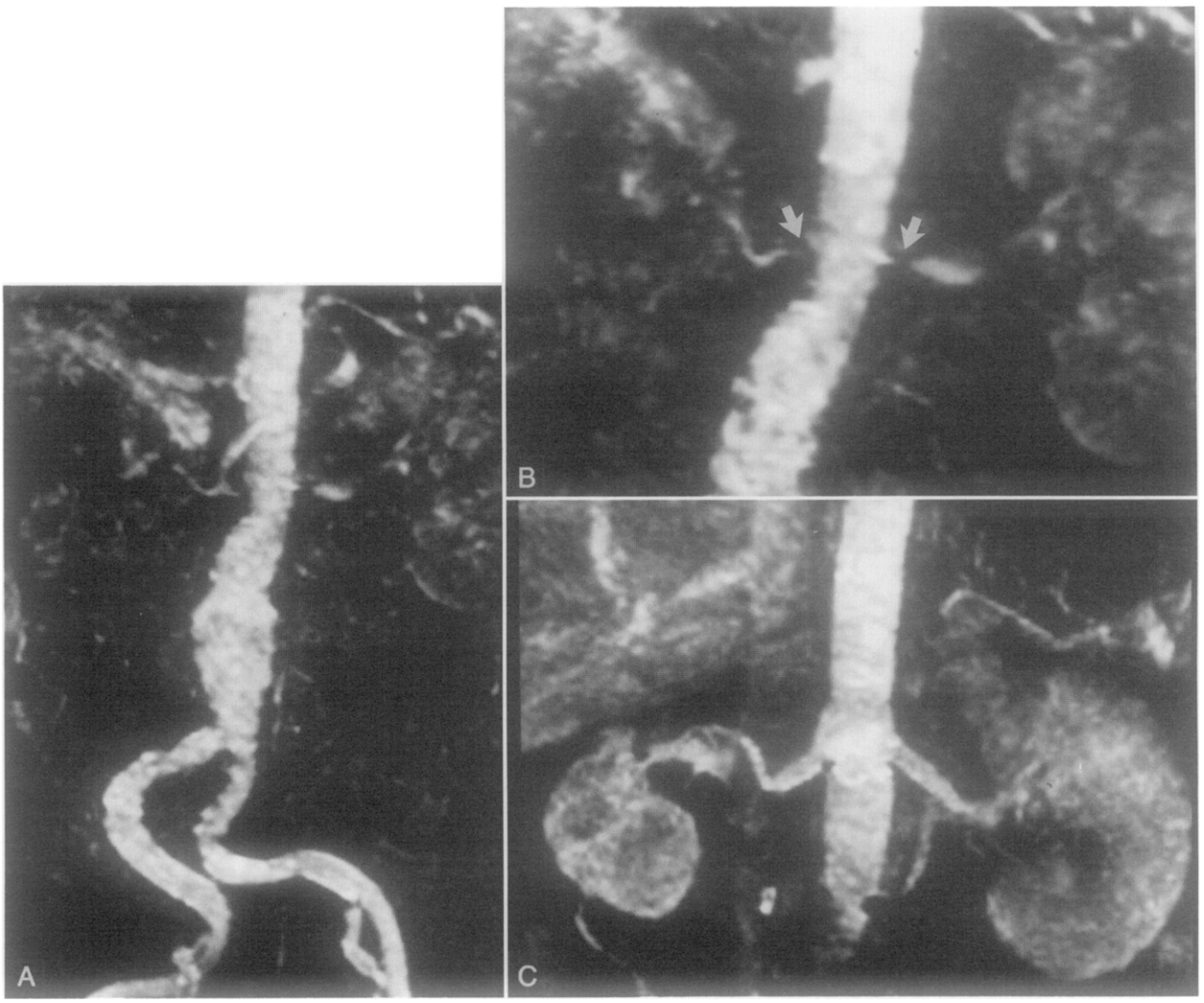

Fig. 9. **(A)** Coronal MIP and **(B)** subvolume MIP of infrarenal AAA with bilateral renal artery stenoses *(arrows)*. After AAA repair with bilateral renal artery endarterectomy (**C**) there is improved visualization of renal arteries and increased renal parenchymal enhancement.

mesenteric artery and internal iliac arteries for occlusive disease has not been a clinical problem. It is important to search carefully at the time of surgery for accessory renal arteries because of the decreased ability of MRA to detect them.[17] In this series, however, the two accessory renal arteries missed by MRA were also missed by angiography. For these reasons, gadolinium-enhanced MRA is becoming the primary imaging modality for preoperative evaluation of AAA at the authors' institution.

Gadolinium-enhanced MRA has certain limitations. It can not be offered to patients with contraindications to MRA, including implanted electronic devices such as pacemakers. Some patients with claustrophobia may refuse the examination or require heavy sedation. We now routinely give 5 to 10 mg diazepam to all patients 30 minutes before MRI. This not only lessens claustrophobia but also reduces cardiac and respiratory motion artifacts. Although MRA can detect most stenoses, renal artery lesions in some patients are not resolved sufficiently to evaluate their hemodynamic and functional importance. Fortunately, gadolinium-enhanced MRA does not interfere with other imaging procedures, so conventional angiography may subsequently be used to evaluate any unresolved anatomic issues. In fact, it is possible to tailor the angiography to answer specific questions, thereby limiting the iodinated contrast dose, procedure time, and degree of catheter manipulation

when the aortic anatomy has already been defined by MRA.

Previously placed metallic surgical clips create artifacts that may obscure arteries (Fig. 3). To maintain future MRA options in patients after operation, such metallic surgical clips should be avoided, particularly in the region of vascular anastomoses. Postoperative scans in five of our patients demonstrated the renal arteries unusually well (Fig. 9). This may be related to several factors. First, much less respiratory or other motion artifact affects the region of the surgical bed when patients are splinting that area for pain relief. Second, postoperative pain medications help to minimize patient motion and intestinal peristalsis. Third, patent renal arteries and grafts of normal caliber are easier to demonstrate than stenotic ones (Fig. 9) because of the intrinsic resolution limits of MRA. Lastly, cardiac output may be decreased after several days in the hospital, a change that would result in transiently higher arterial gadolinium concentrations for the same gadolinium infusion rates.[16]

Gadolinium-enhanced MRA is still early in its development and technological advances are occurring at a rapid pace. Improved magnets will provide higher field strength, better field uniformity, faster gradients, and specialized coils that will increase the image signal-to-noise ratio. These improvements will permit higher resolution imaging. Pulse sequences are being developed to include mechanisms for better suppression of background tissue signal and to further reduce motion artifacts. Phase contrast techniques have the potential to provide quantitative information about blood flow[30] in addition to providing anatomic images. There is also the possibility of assessing organ perfusion by measuring the degree of gadolinium enhancement. This may better define the significance of stenoses once they are identified. Higher doses of gadolinium and gadolinium chelates with higher relaxivity may also improve image quality.

Although the current technology is new and evolving, gadolinium-enhanced MRA now can provide anatomic information for planning aortic reconstructions in patients with AAA. At centers with MRA expertise, it is no longer necessary to routinely subject patients to the nephrotoxic effects of iodinated contrast before AAA operations. Conventional angiography can be reserved for selected cases when specific questions are not adequately resolved by MRA.

Table I. Characteristics of AAA

	No.
Suprarenal	11
Pararenal	6
Juxtarenal	6
Infrarenal	20
Mean diameter	5.4 (3-8.7)* cm
Thrombus	35 (81%)
Inflammatory AAA	1 (2%)
Leaking AAA	1 (2%)
Retroaortic renal vein	6 (14%)
Accessory renal arteries	5 (12%)

*Minimum-maximum.

We thank Drs. Aisen, Cohan, Kaufman, Quint, Deeb, Francis, Chenevert, Greenfield, Strouse, Bass, Pfammeter, and all the MR fellows for helpful suggestions. We also thank all of the MR, CT, Ultrasound, and Angio technologists, as well as Jennifer Ward and Frank Londy for technical and research assistance, and Karen Travis for assistance with preparation of the manuscript. The provision of infusion pumps from Abbott Laboratories and Redington Medical Technologies is appreciated.

REFERENCES

1. Lee JK, Ling D, Heiken JP, et al. Magnetic resonance imaging of abdominal aortic aneurysms. Am J Roentgenol 1984;143-1197-202.
2. Flak B, Li OK, Ho BY, et al. Magnetic resonance imaging of aneurysms of the abdominal aorta. Am J Roentgenol 1985; 144:991-6.
3. Rapp JH, Pan XM, Hale J, et al. "Angiography" by magnetic resonance imaging: detailed vascular anatomy without ionizing radiation or contrast media. Surgery 1989;105: 662-7.
4. Koslin DB, Kenney PJ, Keller FS, Koehler RE, Gross GM. Preoperative evaluation of abdominal aortic aneurysm by MR imaging with aortography correlation. Cardiovasc Intervent Radiol 1988;11:329-35.
5. Kandarpa K, Piwnica-Worms D, Chopra PS, et al. Prospective double-blinded comparison of MR imaging and aortography in the preoperative evaluation of abdominal aortic aneurysms. J Vasc Interv Radiol 1992;3:83-9.
6. Arlart IP, Guhl L, Edelman RR. Magnetic resonance angiography of the abdominal aorta. Cardiovasc Intervent Radiol 1992;15:43-50.
7. Lewin JS, Laub G, Hausmann R. Three-dimensional time-of-flight MR angiography: applications in the abdomen and thorax. Radiology 1991;179:261-4.
8. Lewin JS. Time-of-flight magnetic resonance angiography of the aorta and renal arteries. Invest Radiol 1992;27(Suppl 2):S84-S89.
9. Roditi GH, Smith FW, Redpath TW. Evaluation of tilted, optimized, non-saturating excitation pulses in 3D magnetic resonance angiography of the abdominal aorta and major branches in volunteers. Br J Radiol 1994;67:11-3.
10. Kim D, Edelman RR, Kent KC, Porter DH, Skillman JJ. Abdominal aorta and renal artery stenosis: evaluation with MR angiography. Radiology 1990;174:727-31.
11. Ecklund K, Hartnell GG, Hughes LA, Stokes KR, Finn JP. MR angiography as the sole method in evaluating abdominal

aortic aneurysms: correlation with conventional techniques and surgery. Radiology 1994;192:345-50.
12. Kaufman JA, Yucel EK, Waltman AC, et al. MR angiography in the preoperative evaluation of abdominal aortic aneurysms: a preliminary study. J Vasc Interv Radiol 1994;5:489-96.
13. Debatin JF, Spritzer CE, Grist TM, et al. Imaging of the renal arteries: value of MR angiography. Am J Roentgenol 1991; 157:981-90.
14. Debatin JF, Sostman HD, Knelson M, Argabright M, Spritzer CE. Renal magnetic resonance angiography in the preoperative detection of supernumerary renal arteries in potential kidney donors. Invest Radiol 1993;28:882-9.
15. Prince MR, Yucel EK, Kaufman JA, Harrison DC, Geller SC. Dynamic gadolinium-enhanced three-dimensional abdominal MR arteriography. J Magn Reson Imaging 1993;3:877-81.
16. Prince MR. Gadolinium-enhanced MR aortography. Radiology 1994;191:155-64.
17. Kaufman JA, Geller SC, Petersen MJ, Cambria RP, Prince MR, Waltman AC. MR imaging (including MR angiography) of abdominal aortic aneurysms: comparison with conventional angiography. Am J Roentgenol 1994;163:203-10.
18. Sivananthan UM, Ridgway JP, Bann K, et al. Fast magnetic resonance angiography using turbo-FLASH sequences in advanced aortoiliac disease. Br J Radiol 1993;66:1103-10.
19. Swedenborg J. Optimal method for imaging of abdominal aortic aneurysms. Ann Chir Gynaecol 1992;81:158-60.
20. LaRoy LL, Cormier PJ, Matalon TA, Patel SK, Turner DA, Silver B. Imaging of abdominal aortic aneurysms. Am J Roentgenol 1989;152:785-92.
21. Ernst CB. Abdominal aortic aneurysm. N Engl J Med 1993;328:1167-72.
22. Bandyk DF. Preoperative imaging of aortic aneurysms: conventional and digital subtraction angiography, computed tomography scanning, and magnetic resonance imaging. Surg Clin North Am 1989;69:721-35.
23. Ruff SJ, Watson MR. Magnetic resonance imaging versus angiography in the preoperative assessment of abdominal aortic aneurysms. Am J Surg 1988;155:651-4.
24. Durham JR, Hackworth CA, Tober JC, et al. Magnetic resonance angiography in the preoperative evaluation of abdominal aortic aneurysms. Am J Surg 1993;166:173-8.
25. Siegel CL, Cohan RH. CT of abdominal aortic aneurysms. Am J Roentgenol 1994;163:17-29.
26. Yucel EK. MR angiography for evaluation of abdominal aortic aneurysm: has the time come? Radiology 1994;192: 321-3.
27. Rubin GD, Walker PJ, Dake MD, et al. Three-dimensional spiral computed tomographic angiography: an alternative imaging modality for the abdominal aorta and its branches. J VASC SURG 1993;18:656-64.
28. Haustein J, Niendorf HP, Krestin G, et al. Renal tolerance of gadolinium-DTPA/dimeglumine in patients with chronic renal failure. Invest Radiol 1992;27:153-6.
29. Rofsky NM, Weinreb JC, Bosniak MA, Libes RB, Birnbaum BA. Renal lesion characterization with gadolinium-enhanced MR imaging: efficacy and safety in patients with renal insufficiency. Radiology 1991;180:85-9.
30. Dumoulin CL, Souza SP, Pelc NJ. Phase-sensitive flow imaging. In: Potchen EJ, Haacke EM, Siebert JE, Gottschalk A. Magnetic Resonance Angiography. St. Louis: Mosby–Year Book, 1993:173-86.

Submitted Oct. 11, 1994; accepted Jan. 5, 1995.

APPENDIX

Detailed imaging parameters are described in this appendix in a form compatible with the GE Signa Magnet, 1.5 T with 5.3 software.

An initial sagittal T_1-weighted spin echo localizer was landmarked just below the xyphoid and obtained by use of the following parameters: (repetition time (TR) = 333 msec, time-to-echo (TE) = 25 msec, bandwidth = 16 kHz, slice thickness = 8 mm (performed as a triple interleave with no gap), respiratory compensation, matrix = 256 by 128 pixels with frequency encoding superior to inferior, a 40 to 48 cm field of view, and 2 NEX (averages). Image acquisition time was 9:35 minutes.

The first gadolinium-enhanced acquisition was a coronal 3D spoiled gradient echo sequence centered on the abdominal aorta and obtained with the following parameters: TR = 24 msec, TE = 6.9 msec, flip angle = 40 degrees, bandwidth = 16 kHz, 28 slices with 2.5 to 2.8 mm slice thickness, matrix = 256 by 256 pixels, frequency encoding superior to inferior, first order gradient moment nulling (flow compensation), field-of-view = 36 cm, 1 NEX. No saturation pulses were used; the total image acquisition time was 3:20 minutes.

The coronal volume was positioned with the top edge at the diaphragm just below the heart and the front edge anterior to the preaortic left renal vein where it passed under the superior mesenteric artery and anterior to the common femoral arteries at the level of the femoral heads. If the posterior edge of the volume did not reach back into the renal parenchyma bilaterally, the slices were made thicker up to a maximum thickness of 2.8 mm. In most cases, this 28-slice coronal volume was too thin to obtain an image of the entire aneurysm; accordingly the anterior margin of the aneurysm was deliberately excluded on this sequence.

Gadolinium was infused during the acquisition to preferentially enhance arteries more than veins in a manner somewhat analogous to spiral CT. The same volume, 42 ml (two vials, 21 mmol/L), gadodiamide (Omniscan; Sanofi Winthrop Pharmaceuticals, New York, NY), gadoteridol (Prohance; Squibb Diagnostics, Princeton, N.J.), or gadopentetate dimeglumine (Magnevist; Berlex Laboratories, Wayne, N.J.) was used in every patient under 95 Kg (210 pounds). Patients weighing greater than 95 Kg were given three vials (63 ml) of gadolinium. The gadolinium infusion was begun simultaneously with image acquisition. The infusion was performed either by hand or with an MRA-compatible infusion pump (Redington Medical Technologies, Inc., East Walpole,

MA). The infusion was completed 60 seconds before scan termination and was immediately followed by a saline solution flush of 10 to 20 ml to ensure delivery of the entire dose of gadolinium. Special care was taken to maintain a high infusion rate during the middle of the acquisition when the center of k-space was acquired.

Immediately after the dynamic gadolinium acquisition, six to eight contiguous, sagittal 2D time-of-flight, spoiled, gradient echo images were acquired, centered on the visceral arteries with the following parameters: TR = 33, TE = minimum (7 msec), flip angle = 45 degrees, bandwidth = 16 kHz, slice thickness = 6 cm, first order gradient moment nulling (flow compensation), matrix = 256 by 192, frequency encoding superior-to-inferior, 36 cm field-of-view, 1 NEX. Each sagittal image was obtained during suspended respiration (7 seconds per breath hold). Immediately after these sagittal images were obtained, axial 2D time-of-flight gradient echo images were obtained in a similar fashion during suspended respiration with the following parameters: TR = 22 msec, TE = minimum full (12 msec), flip angle = 60 degrees, bandwidth = 16 kHz, slice thickness = 8 mm with a 5 mm interslice gap, matrix = 256 by 256, 28 to 32 cm field-of-view, 2 NEX, first order gradient moment nulling (flow compensation), and no phase wrap. In patients who could not hold their breath, respiratory compensation was used and the NEX was increased to 4. The axial images covered from above the celiac trunk to below the AAA. If the iliac arteries were aneurysmal, the axial 2D time-of-flight images were extended down into the pelvis.

After the time-of-flight images, an axial 3D phase contrast volume was acquired centered on the renal arteries with the following parameters: TR = 24 msec, TE = 7.7 msec, flip angle = 45 degrees, bandwidth = 16 kHz, field-of-view = 32 cm, 28 slices with 2.5 mm slice thickness, flow compensation, no phase wrap, matrix = 256 by 128, frequency encoding right-left, 32 cm field-of-view, 2 NEX with velocity encoding in all directions at 30 cm/sec. The image acquisition time was 13:07 minutes. Images were reconstructed with the phase difference method illustrating maximum velocity in all flow directions, as well as right-to-left flow to evaluate the retrocaval course of the right renal artery. In patients suspected of having very slow renal artery flow, such as patients with a serum creatinine greater than 3 mg/dl, the velocity encoding was reduced to 20 cm/sec.

Images were reconstructed by a vascular radiologist using a computer workstation (GE Medical Systems). Subvolume maximum intensity projections (MIPs) and single voxel thick reformations were made through the origins of each of the major aortic branch vessels. The subvolume MIPs were made by reviewing the raw data images to identify the minimum number of images required to demonstrate the renal arteries and then collapsing these into a single coronal image. This was similarly performed for the aortoiliac system. A sagittal subvolume MIP was performed centered on the celiac and superior mesenteric arteries for both the dynamic gadolinium-enhanced coronal sequence and for the sagittal 2D TOF sequence.